

DYNAMICS AND PATH-TRACKING CONTROL OF AN UNMANNED BICYCLE

Chih-Keng Chen

Department of Mechanical and Automation
Engineering
Da-Yeh University
112 Shan-Jiau Rd., Changhua, Taiwan 515 R.O.C
E-mail: ckchen@mail.dyu.edu.tw
TEL: 886-4-8511888 ext. 2108
FAX: 886-4-8511224

Thanh-Son Dao

Department of Mechanical and Automation
Engineering
Da-Yeh University
112 Shan-Jiau Rd., Changhua, Taiwan 515 R.O.C
E-mail: r9201001@mail.dyu.edu.tw

ABSTRACT

Due to its non-holonomic constraints and its highly unstable nature, the unmanned bicycle is difficult to be controlled for tracking a target path while retaining balance. As a result of the non-holonomic constraint conditions, the instantaneous velocity of the vehicle is limited to certain directions. Constraints of this kind occur under the no-slip condition. In this paper, the equations of motion describing the motions of the bicycle are developed using Lagrange's equations for quasi-coordinates. Pure rolling without slip constraints between the ground and the two wheels are also considered in this model. Based on the developed equations of motion, two strategies for path-tracking control of an unmanned bicycle are proposed, compared and discussed.

Keywords - Bicycle Dynamics, Multibody Systems, Non-holonomic, Path-tracking, Fuzzy Control.

INTRODUCTION

The bicycle is a very common and efficient mean of transportation and is known to be a highly nonlinear system which has interesting non-trivial behaviors. Anyone who has ridden a bicycle has had some practical experience in bicycle stability. The bicycle is not as simple as people thought it would be. Knowledge of bicycle dynamics is of interest to many people. Though controlling a bicycle by human-power is possible for almost everyone, yet dealing with an unmanned bicycle proves to be rather demanding. The challenges in fully understanding bicycle dynamics and control have been attracting considerable attention from a number of researchers in the fields of physics, automation and control. To understand the nature of the dynamics and stability of a bicycle, Johns [1] did a variety of investigations on his bicycle model. He pointed

out that, in order to balance a ridden bicycle, an enough centrifugal force could be generated to correct its fall by steering the fork into the direction of the fall. This theory was well formalized mathematically by Timoshenko et al. [2] and is certainly confirmed by our bicycle riding experience. Schwab et al. [3] developed linearized equations of motion for a bicycle as a benchmark. In their study, the results obtained by pencil-and-paper, the numerical multibody dynamics program SPACAR and the symbolic software AutoSim were compared.

Control efforts for unmanned bicycles have also been addressed in previous studies. Beznos et al. [4] modeled a bicycle with gyroscopes that enabled the vehicle to stabilize itself in an autonomous motion along a straight line as well as along a curve. Han et al. [5] derived a simple kinematic and dynamic formulation of an unmanned electric bicycle. The controllability of the stabilization problem was also checked and a control algorithm for self-stabilization of the vehicle with bounded wheel speed and steering angle using nonlinear control was proposed. Yavin [6] dealt with the stabilization and control of a riderless bicycle by a pedalling torque, a directional torque and a rotor mounted on the crossbar that generated a tilting torque. Getz et al. [7, 8] derived a controller using steering and rear-wheel torque to recover the balance of their bicycle from a near fall as well as to converge to a time-parameterized path in the ground plane. In another study [9], Getz applied internal equilibrium control to the problem of path-tracking with balance for the bicycle. From the internal dynamics of the bicycle, an internal equilibrium manifold, a submanifold of the state-space, was constructed. Recently, some researchers have even added a balance mass to their electric bicycle system [10] or utilized fuzzy and intelligent control [11] for the stabilization and path-tracking problems.

Most previous studies have dealt with simplified mathematical bicycle models, which were subsequently used to implement simulations, analysis and experiments. However, due to their simplicity, the mathematical models were incapable of presenting all of the dynamic motions of the system in certain situations. With that in mind, we approach the problem by modeling the bicycle as a nine-degree-of-freedom-(DOF) system in three-dimensional space using Lagrange's equations for quasi-coordinates. The constraint conditions of the two wheels are also considered. The developed equations of motion are then used to derive controllers, including PID and fuzzy ones. With these control laws, our concern is not only to stabilize the vehicle but also to control it to track a desired trajectory and roll-angle, which was also suggested by Getz [9] and Berriah et al. [12]; however, they used much simpler models and different approaches.

This study investigates the dynamics governing a bicycle and then designs controllers for path-tracking problem. Implementation of this research draws upon several areas of dynamic systems and control engineering: holonomic and non-holonomic constraints, unstable system analysis, PID and fuzzy controller design, and nonlinear control. Therefore, the bicycle problem is an excellent example of dynamics and nonlinear control.

DYNAMIC MODEL

The dynamics and stability of two-wheeled vehicles were studied extensively by Sharp [13, 14] using motorcycle models, which are mainly different from bicycles in the vehicle mass and the presence of suspensions. By assuming that the motorcycle was running straight on a flat, level road surface and the rider was a rigid body fixed to the rear frame, Sharp introduced the wobble and the weave modes that cause the low-frequency oscillation of the front and the rear parts. He stated that the wobble mode was influenced by the weight and speed of the vehicle and the weave mode had a natural frequency increasing at high forward speeds. From Sharp's point of view, we will ignore the weave and the wobble modes for the unmanned bicycle due to its light weight and relatively low speed range.

In this section, the compact equations of motion with nine degrees of freedom are developed to describe the dynamics of the bicycle. The equations discussed here are developed using Lagrange's equations for quasi-coordinates. The pure rolling constraints between the ground and the wheels are considered in the dynamic equations of the bicycle system. However, in this paper we will not discuss in detail about bicycle dynamics, the readers should refer to [15] for further discussion about bicycle dynamics and associated problems such as constraint conditions for two wheels, equilibrium, algorithm for searching equilibrium points and radii of curvatures of the bicycle in turning.

Coordinate Systems

The schematic bicycle model is shown in Fig. 1. Let the uppercase letters A , B , D and F represent the vehicle body, the rear wheel, the front wheel and the fork, respectively, while the lowercase ones a , b , d , and f are used to designate the center of mass of each part. Reference point c is between the saddle and the vehicle body; e is a point between the vehicle body and the front fork; o' and s are the contact points between the ground and the rear and front wheels, respectively.

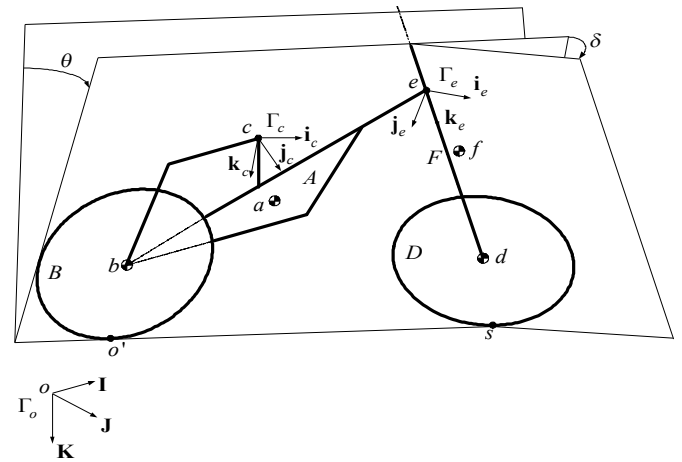


Fig. 1 Schematic of a bicycle.

There are three SAE-standard coordinate systems used in the bicycle model: (1) an inertial frame $\Gamma_o(\mathbf{I}, \mathbf{J}, \mathbf{K})$ fixed on the ground, (2) a reference frame $\Gamma_c(\mathbf{i}_c, \mathbf{j}_c, \mathbf{k}_c)$ mounted on the model at point c , and (3) a frame $\Gamma_e(\mathbf{i}_e, \mathbf{j}_e, \mathbf{k}_e)$ placed on the front fork at point e . The coordinate Γ_e is obtained by rotating about Γ_c a rake and a steering angle as shown in Fig. 1. In this paper the dynamics of the bicycle is described by the motion of the reference point c . Six coordinates are used to signify the positions and orientations of point c . The other three coordinate variables are the rotating angles of the front and rear wheels and the steering angle of the front fork. According to the foregoing definitions, the generalized coordinates $\mathbf{q} \in \mathbb{R}^9$ can be written as

$$\mathbf{q} = [X \ Y \ Z \ \psi \ \phi \ \theta \ \delta \ \phi_f \ \phi_r]^T, \quad (1)$$

where (X, Y, Z) are the position parameters and (ψ, ϕ, θ) are the Euler angles, which describe the relative position and orientation between the coordinates Γ_c and Γ_o ; $\delta \in \mathbb{R}$ is the steering angle; ϕ_f and $\phi_r \in \mathbb{R}$ are the rotating angles of the front and rear wheels, respectively. The velocity vector $\mathbf{u} \in \mathbb{R}^9$ is

$$\mathbf{u} = [v_x \ v_y \ v_z \ \omega_x \ \omega_y \ \omega_z \ \dot{\delta} \ \dot{\phi}_r \ \dot{\phi}_f]^T, \quad (2)$$

the components of which are quasi-velocities (generalized speeds).

Dynamics of Nine-DOF Model

For simplicity, the position vector, the velocity and angular velocity of body M in frame Γ_n will be denoted by \mathbf{r}_M^n , \mathbf{v}_M^n and $\boldsymbol{\omega}_M^n$, respectively.

To develop the dynamic equations of motion of a bicycle system, we first need to write down the kinetic and potential energies of the system. The kinetic energies of all parts can be written in terms of their centers of mass as

$$\begin{aligned} T_A &= \frac{1}{2} m_a (\mathbf{v}_a^c)^T \mathbf{v}_a^c + \frac{1}{2} (\boldsymbol{\omega}_A^c)^T \mathbf{I}_A \boldsymbol{\omega}_A^c, \\ T_B &= \frac{1}{2} m_b (\mathbf{v}_b^c)^T \mathbf{v}_b^c + \frac{1}{2} (\boldsymbol{\omega}_B^c)^T \mathbf{I}_B \boldsymbol{\omega}_B^c, \\ T_F &= \frac{1}{2} m_f (\mathbf{v}_f^c)^T \mathbf{v}_f^c + \frac{1}{2} (\boldsymbol{\omega}_F^c)^T \mathbf{I}_F \boldsymbol{\omega}_F^c, \\ T_D &= \frac{1}{2} m_d (\mathbf{v}_d^c)^T \mathbf{v}_d^c + \frac{1}{2} (\boldsymbol{\omega}_D^c)^T \mathbf{I}_D \boldsymbol{\omega}_D^c, \end{aligned} \quad (3)$$

where T_A , T_B , T_F and $T_D \in \mathbb{R}$ are the kinetic energies of the bicycle body, the rear wheel, the fork and the front wheel, respectively; \mathbf{I}_A , \mathbf{I}_B , \mathbf{I}_F and $\mathbf{I}_D \in \mathbb{R}^{3 \times 3}$ are the inertia matrices of corresponding bodies. The mass of each part and geometrical values are listed in Table 1a. In Table 1b are the moments of inertia of the vehicle body, front fork and the two wheels. All these numerical values were measured from a real bicycle system. The total kinetic energy is obtained by summing all the kinetic energies of all parts, thereby resulting in

$$T = T_A + T_B + T_F + T_D = \frac{1}{2} \mathbf{u}^T \mathbf{J} \mathbf{u}, \quad (4)$$

where $\mathbf{J} \in \mathbb{R}^{9 \times 9}$ is the inertia matrix of the system.

The potential energy $V \in \mathbb{R}$ has the form

$$V = mgh, \quad (5)$$

or,

$$V = -\mathbf{g}_3^T (m_a \mathbf{r}_a^o + m_b \mathbf{r}_b^o + m_f \mathbf{r}_f^o + m_d \mathbf{r}_d^o), \quad (6)$$

where $\mathbf{g}_3 = [0 \ 0 \ g]^T$ and \mathbf{r}_a^o , \mathbf{r}_b^o , \mathbf{r}_f^o and \mathbf{r}_d^o are position vectors of all parts of the bicycle.

The generalized velocities $\dot{\mathbf{q}}$ are related to the quasi-velocities \mathbf{u} by

$$\mathbf{u} = \mathbf{Y} \dot{\mathbf{q}}, \quad \text{or} \quad \dot{\mathbf{q}} = \mathbf{W} \mathbf{u}, \quad (7)$$

where \mathbf{Y} and $\mathbf{W} \in \mathbb{R}^{9 \times 9}$ are transform matrices defined by

$$\mathbf{Y} = \begin{bmatrix} \mathbf{R} & \mathbf{0} & \mathbf{0} \\ \mathbf{0} & \mathbf{S} & \mathbf{0} \\ \mathbf{0} & \mathbf{0} & \mathbf{I} \end{bmatrix}, \quad \mathbf{W} = \mathbf{Y}^{-1} = \begin{bmatrix} \mathbf{R}^T & \mathbf{0} & \mathbf{0} \\ \mathbf{0} & \mathbf{S}^{-1} & \mathbf{0} \\ \mathbf{0} & \mathbf{0} & \mathbf{I} \end{bmatrix}, \quad (8)$$

and $\dot{\mathbf{q}} = [\dot{X} \ \dot{Y} \ \dot{Z} \ \dot{\psi} \ \dot{\phi} \ \dot{\theta} \ \dot{\delta} \ \dot{\phi}_r \ \dot{\phi}_f]^T$.

Lagrange's equations for quasi-coordinates [16] can be formulated as

$$\frac{d}{dt} \left(\frac{\partial T}{\partial \dot{\mathbf{u}}} \right) + \frac{\partial T}{\partial \mathbf{u}} \boldsymbol{\Delta} - \frac{\partial T}{\partial \mathbf{q}} \mathbf{W} + \frac{\partial V}{\partial \mathbf{q}} \mathbf{W} = \mathbf{U}_{nc}^T, \quad (9)$$

where $\frac{\partial T}{\partial \mathbf{u}} = \mathbf{u}^T \mathbf{J}$, $\frac{d}{dt} \left(\frac{\partial T}{\partial \dot{\mathbf{u}}} \right) = \dot{\mathbf{u}}^T \mathbf{J} + \mathbf{u}^T \dot{\mathbf{J}}$, and

$\mathbf{U}_{nc} = \mathbf{W}^T \mathbf{Q}_{nc} \in \mathbb{R}^9$ are the non-conservative forces. The coefficient matrix $\boldsymbol{\Delta} \in \mathbb{R}^{9 \times 9}$ is

$$\boldsymbol{\Delta} = \left(\dot{\mathbf{Y}} - \frac{\partial \mathbf{u}}{\partial \dot{\mathbf{q}}} \right) \mathbf{W} = \left(\frac{d}{dt} \frac{\partial \mathbf{u}}{\partial \dot{\mathbf{q}}} - \frac{\partial \mathbf{u}}{\partial \mathbf{q}} \right) \mathbf{W}, \quad (10)$$

where $\frac{\partial \mathbf{u}}{\partial \dot{\mathbf{q}}} = \left[\frac{\partial \mathbf{u}}{\partial \dot{q}_1}, \dots, \frac{\partial \mathbf{u}}{\partial \dot{q}_9} \right] \in \mathbb{R}^{9 \times 9}$.

Table 1. Simulation parameters.
(a)

Name	Value	Name	Value
m_a	11.05(kg)	m_b	2.09(kg)
m_d	3.92(kg)	m_f	4.04(kg)
$\boldsymbol{\rho}_a$	(0.1296, 0,0.285)	$\boldsymbol{\rho}_b$	(-0.365, 0,0.503)
$\boldsymbol{\rho}_d$	(0, 0,0.601)	$\boldsymbol{\rho}_e$	(-0.789, 0,0.078)
$\boldsymbol{\rho}_f$	(0.017, 0,0.1083)	r	0.325(m)
g	9.80665(m/s ²)	ε	15°

(b)

	Moment of Inertia (kg-m ²)
Vehicle Body	$\mathbf{I}_a = \begin{bmatrix} 0.407 & 0 & -0.068 \\ & 1.934 & 0 \\ & & 1.558 \end{bmatrix}$
Front Fork	$\mathbf{I}_f = \begin{bmatrix} 0.421 & 0 & -0.025 \\ & 0.384 & 0 \\ & & 0.041 \end{bmatrix}$
Wheels	$\mathbf{I}_b = \begin{bmatrix} 0.109 & 0 & 0 \\ & 0.218 & 0 \\ & & 0.109 \end{bmatrix}; \mathbf{I}_d = \begin{bmatrix} 0.204 & 0 & 0 \\ & 0.408 & 0 \\ & & 0.204 \end{bmatrix}$

One can rewrite Eq. (9) in the standard form of differential equations as

$$\mathbf{J}\dot{\mathbf{u}} = -\mathbf{J}\mathbf{u} - \Delta^T \mathbf{J}\mathbf{u} + \mathbf{W}^T \left(\frac{\partial T}{\partial \mathbf{q}} \right)^T - \mathbf{W}^T \left(\frac{\partial V}{\partial \mathbf{q}} \right)^T + \mathbf{U}_{nc}, \quad (11)$$

or simply,

$$\mathbf{J}\dot{\mathbf{u}} = \mathbf{Q}. \quad (12)$$

Constraint Conditions for Wheels

By considering that the front and rear wheels of the bicycle roll without slipping, eight constraint equations, including four holonomic and four non-holonomic ones, can be found. For the rear wheel, there are two holonomic constraints, which are [15]

$$Z - \sin \phi (x_b - r \sin \alpha_r) + \cos \phi \cos \theta (z_b + r \cos \alpha_r) = 0, \quad (13)$$

and

$$\cos \phi \cos \theta \sin \alpha_r - \sin \phi \cos \alpha_r = 0; \quad (14)$$

and two non-holonomic constraints, which are [15]

$$v_{o'_x} (\cos \psi \cos \phi) + v_{o'_y} (\cos \psi \sin \phi \sin \theta - \sin \psi \cos \theta) + v_{o'_z} (\cos \psi \sin \phi \cos \theta + \sin \psi \sin \theta) = 0, \quad (15)$$

and

$$v_{o'_x} (\sin \psi \cos \phi) + v_{o'_y} (\sin \psi \sin \phi \sin \theta + \cos \psi \cos \theta) + v_{o'_z} (\sin \psi \sin \phi \cos \theta - \cos \psi \sin \theta) = 0; \quad (16)$$

where $\alpha_r \in \mathbb{R}$ is the included angle between $\mathbf{R}_r \in \mathbb{R}^3$, the position vector of the contact point o' relative to the center of mass b of the wheel, and vector $\mathbf{k}_c \in \mathbb{R}^3$ as shown in Fig. 2; $r \in \mathbb{R}$ is the radius of the two wheels.

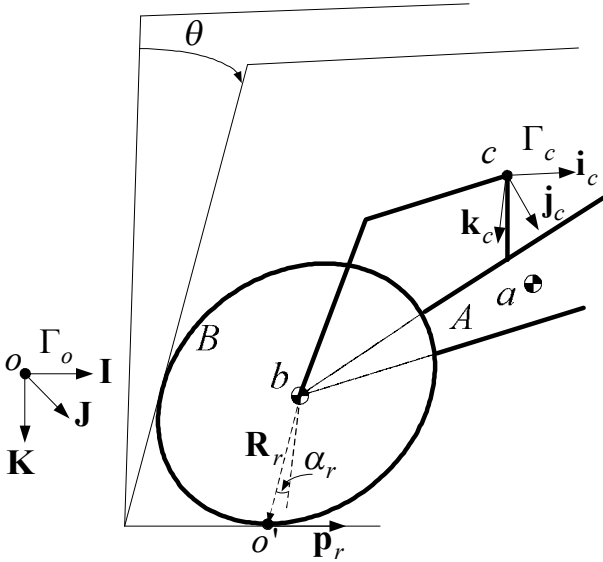


Fig. 2 Schematic of rear wheel.

Similarly, for the front wheel, there are also two holonomic constraints formulated by [15]

$$\begin{aligned} & Z - x_e \sin \phi + z_e \cos \phi \cos \theta + z_d (-\sin \phi \sin \varepsilon + \cos \phi \cos \theta \cos \varepsilon) \\ & + x_d (-\sin \phi \cos \delta \cos \varepsilon + \cos \phi \sin \theta \sin \delta - \cos \phi \cos \theta \cos \delta \sin \varepsilon) \\ & + r \sin \alpha_f (-\cos \phi \sin \theta \sin \delta + \cos \phi \cos \theta \cos \delta \sin \varepsilon + \sin \phi \cos \delta \cos \varepsilon) \\ & + r \cos \alpha_f (-\sin \phi \sin \varepsilon + \cos \phi \cos \theta \cos \varepsilon) = 0, \end{aligned} \quad (17)$$

and

$$\begin{aligned} & (\cos \phi \sin \theta \sin \delta - \cos \phi \cos \theta \cos \delta \sin \varepsilon - \sin \phi \cos \delta \cos \varepsilon) \cos \alpha_f \\ & + (\cos \phi \cos \theta \cos \varepsilon - \sin \phi \sin \varepsilon) \sin \alpha_f = 0; \end{aligned} \quad (18)$$

and two non-holonomic constraints defined by [15]

$$\begin{aligned} & v_{sx} \cos \psi \cos \phi + v_{sy} (\cos \psi \sin \phi \sin \theta - \sin \psi \cos \theta) + \\ & + v_{sz} (\cos \psi \sin \phi \cos \theta + \sin \psi \sin \theta) = 0, \end{aligned} \quad (19)$$

and

$$\begin{aligned} & v_{sx} \sin \psi \cos \phi + v_{sy} (\sin \psi \sin \phi \sin \theta + \cos \psi \cos \theta) + \\ & + v_{sz} (\sin \psi \sin \phi \cos \theta - \cos \psi \sin \theta) = 0; \end{aligned} \quad (20)$$

where $\alpha_f \in \mathbb{R}$ is the included angle between $\mathbf{R}_f \in \mathbb{R}^3$, the position vector of the contact point s relative to the center of mass d , and vector $\mathbf{k}_e \in \mathbb{R}^3$ as shown in Fig. 3.

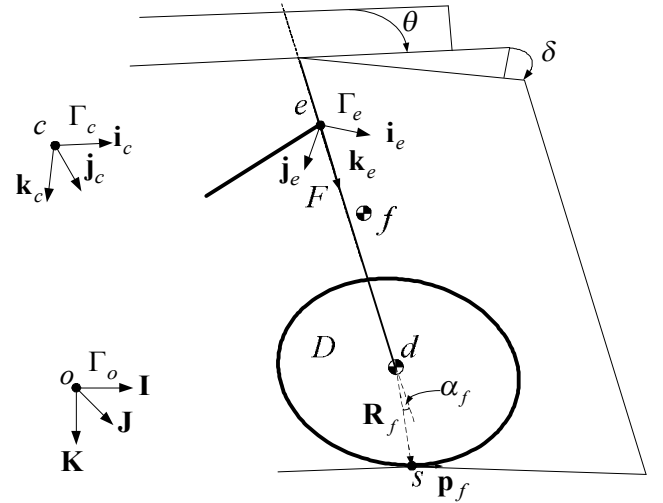


Fig. 3 Schematic of front wheel.

Equations of Motion with Constraints

As a result, eight constraints have been obtained in Eqs. (13)~(20) (see [15]). Among these, there are four holonomic and four non-holonomic constraints. To derive the constraint equations, two algebraic variables, α_r and α_f , have been introduced. Hence, the generalized coordinates and velocity vectors are expanded to $\mathbf{q}_e \in \mathbb{R}^{11}$ and $\mathbf{U} \in \mathbb{R}^{11}$, respectively, as follows

$$\begin{aligned} \mathbf{q}_e &= [X \ Y \ Z \ \psi \ \phi \ \theta \ \delta \ \phi_r \ \phi_f \ \alpha_r \ \alpha_f]^T, \\ \mathbf{U} &= [v_x \ v_y \ v_z \ \omega_x \ \omega_y \ \omega_z \ \dot{\delta} \ \dot{\phi}_r \ \dot{\phi}_f \ \dot{\alpha}_r \ \dot{\alpha}_f]^T. \end{aligned} \quad (21)$$

Differentiating all the holonomic constraints to yield their velocity forms which, with other non-holonomic constraints, can be written as

$$\mathbf{B}\mathbf{U} = \mathbf{0}, \quad (22)$$

where $\mathbf{B} \in \mathbb{R}^{8 \times 11}$ is usually referred to as the constraint Jacobian matrix. All the rows of \mathbf{B} are assumed to be linearly independent. The equations of motion with constraint conditions then become

$$\begin{cases} \dot{\mathbf{q}}_e = \mathbf{W}_e \mathbf{U} \\ \mathbf{J}_e \dot{\mathbf{U}} = \mathbf{Q}_e + \boldsymbol{\tau} - \mathbf{B}^T \boldsymbol{\lambda} \\ \mathbf{B}\mathbf{U} = \mathbf{0} \end{cases} \quad (23)$$

where $\mathbf{W}_e \in \mathbb{R}^{11 \times 1}$ is defined as $\begin{bmatrix} \mathbf{W} & \mathbf{0} & \mathbf{0} \\ \mathbf{0} & \mathbf{1} & \mathbf{0} \\ \mathbf{0} & \mathbf{0} & \mathbf{1} \end{bmatrix}$, $\mathbf{J}_e \in \mathbb{R}^{11 \times 11}$ is

defined as $\begin{bmatrix} \mathbf{J} & \mathbf{0} & \mathbf{0} \\ \mathbf{0} & \mathbf{0} & \mathbf{0} \\ \mathbf{0} & \mathbf{0} & \mathbf{0} \end{bmatrix}$, $\mathbf{Q}_e = \begin{bmatrix} \mathbf{Q} \\ \mathbf{0} \end{bmatrix} \in \mathbb{R}^{11}$ is vector of applied

forces, $\boldsymbol{\lambda} \in \mathbb{R}^8$ represents the Lagrange multipliers or constraint forces coupled to the system by the constraint Jacobian matrix \mathbf{B} , and $\boldsymbol{\tau} \in \mathbb{R}^{11}$ is the generalized non-conservative force vector.

Equation (23) can be solved in a number of ways, some of which are the coordinate reduction [17] and embedding [18] methods. The coordinate reduction method eliminates the Lagrange multipliers by multiplying both sides of $\mathbf{J}_e \dot{\mathbf{U}} = \mathbf{Q}_e + \boldsymbol{\tau} - \mathbf{B}^T \boldsymbol{\lambda}$ by the orthogonal complement matrix $\mathbf{T} \in \mathbb{R}^{3 \times 11}$ of matrix \mathbf{B} so that $\mathbf{T}\mathbf{B}^T = \mathbf{0}$. The coordinate reduction method ultimately reduces the dimension of Eq. (23) to $11 - 8 = 3$. Using a different approach, the embedding method deals with the undetermined multipliers and reduces the equations of motion to minimum dimension by partitioning matrix \mathbf{B} so that $\mathbf{B}_i \dot{\mathbf{U}}_i + \mathbf{B}_d \dot{\mathbf{U}}_d = \mathbf{g}_c$ where $[\mathbf{B}_i | \mathbf{B}_d] = \mathbf{B}$,

$$\mathbf{g}_c = -\dot{\mathbf{B}}\mathbf{U} \text{ and } \mathbf{U} = \begin{bmatrix} \mathbf{U}_i \\ - \\ \mathbf{U}_d \end{bmatrix} \text{ where } \mathbf{U}_i \text{ and } \mathbf{U}_d \text{ are the velocity}$$

arrays of independent and dependent coordinates, respectively. The embedding method then gives

$$\dot{\mathbf{U}} = \begin{bmatrix} \dot{\mathbf{U}}_i \\ \dot{\mathbf{U}}_d \end{bmatrix} = \begin{bmatrix} \mathbf{I} \\ -\mathbf{B}_d^{-1} \mathbf{B}_i \end{bmatrix} \dot{\mathbf{U}}_i + \begin{bmatrix} \mathbf{0} \\ \mathbf{B}_d^{-1} \mathbf{g}_c \end{bmatrix}, \text{ which, when introduced}$$

into Eq. (23) yields $\mathbf{A}\dot{\mathbf{U}}_i = \mathbf{D}$ where $\mathbf{A} = \mathbf{B}_{di}^T \mathbf{J}_e \mathbf{B}_{di}$,

$$\mathbf{D} = \mathbf{B}_{di}^T (\mathbf{Q}_e - \mathbf{J}_e \mathbf{g}_{dc}), \mathbf{B}_{di} = \begin{bmatrix} \mathbf{I} \\ -\mathbf{B}_d^{-1} \mathbf{B}_i \end{bmatrix} \text{ and } \mathbf{g}_{dc} = \begin{bmatrix} \mathbf{0} \\ \mathbf{B}_d^{-1} \mathbf{g}_c \end{bmatrix}.$$

To ensure numerical stability of the governing equations of motion when integrated to yield the time history of the system, the Baumgarte [19] or post-stabilization [20] techniques can be employed.

BALANCING AND ROLL-ANGLE TRACKING

Before the path-tracking strategies can be applied, we first need to design controllers for balancing the bicycle and control it to track a desired roll-angle. With the developed dynamic equations of motion, the unmanned bicycle can be balanced by using the scheme given in Fig. 4. Our bicycle riding experience shows that, the bicycle can be balanced by generating an appropriate steering torque to steer the fork into the direction of fall which was also proposed by Tanaka et al. [21]. In Fig. 4, this steering torque is denoted by $\tau_s \in \mathbb{R}$. The only PID controller in this diagram is to generate the steering torque based on the difference between the desired steering angle δ_{ref} and the measured steering angle δ . To generate appropriate reference steering angle δ_{ref} , a fuzzy controller (designated by FIS_{δ}) is used. The fuzzy controller FIS_{δ} uses two inputs: the measured roll-angle θ and its change $\Delta\theta$ to regulate the steering angle until the bicycle turns to the up-right position.

For roll-angle tracking control, another fuzzy controller, denoted by FIS_{δ_a} , is added. Denote the difference between the desired roll-angle θ_{ref} and the actual roll-angle θ by e_{θ} . The controller FIS_{δ_a} tries to minimize e_{θ} and its change Δe_{θ} by creating an additional angle δ_a as shown in Fig. 4.

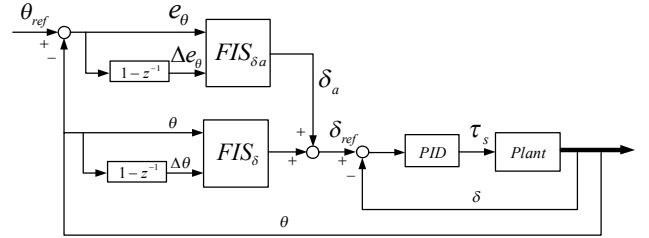
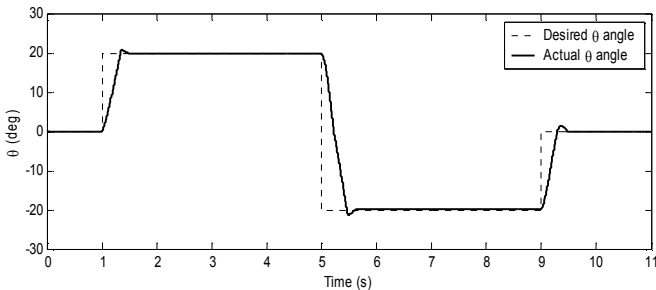


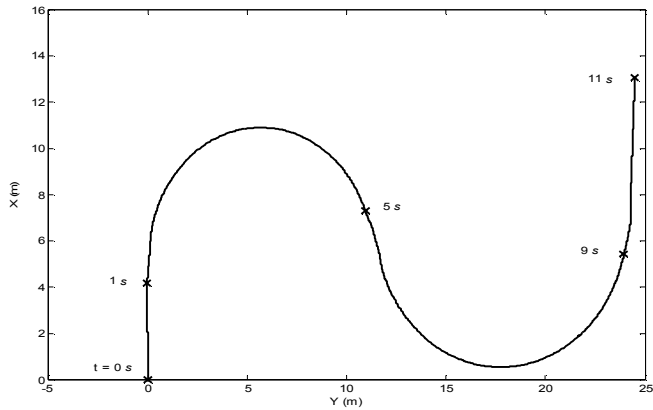
Fig. 4 Balancing and roll-angle tracking scheme.

With this scheme, the balancing and roll-angle tracking tasks can be accomplished. A number of simulations were implemented to show the effectiveness of the designed controllers, one of which is shown in Fig. 5. In this simulation, the bicycle is controlled to track a varying roll-angle while retaining balance. The target roll-angle is initially 0° , then is changed to 20° after 1 second, -20° after 5 seconds and finally 0° after 9 seconds. The time response of θ and the trajectory of the reference point c on the ground plane are shown in Fig. 5a and Fig. 5b, respectively. The ground contact paths of the two wheels are shown in Fig. 5c. The paths of the wheel contact at the start of each turn may be seen to first turn out, then in toward the target direction. This ground path motion is the result of countersteering, the turning of the front wheel in the direction opposite the direction one wishes to go at the start of the turn. Note that countersteering comes naturally out of the controller, as it must for stable turn.

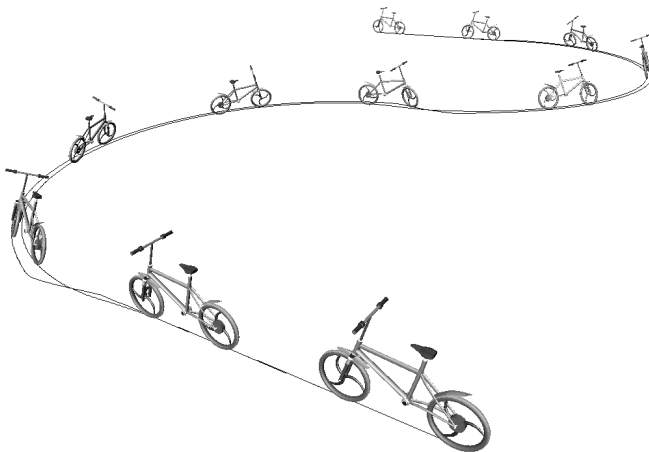
In this paper, we will not discuss deeply in balancing and roll-angle tracking controller design but focus on ground-path tracking problem for the unmanned bicycle with non-holonomic constraints. With the scheme shown in Fig. 4, path-tracking control can be implemented.



(a)



(b)



(c)

Fig. 5 Time response of (a) roll-angle, (b) resulting trajectory of reference point c on ground plane and (c) ground contact paths of two wheels for tracking a varying θ angle.

PATH-TRACKING STRATEGIES

Due to its non-holonomic constraints and highly unstable nature, the bicycle is difficult to be controlled for tracking a given path while retaining balance. As a result of the non-holonomic constraints condition, the instantaneous velocity of the vehicle is limited to certain directions. Constraints of this kind occur under the rolling and no-slip conditions. To have a good understanding of bicycle dynamics and control, two strategies for path-tracking for the unmanned bicycle are proposed and discussed in this section.

For bicycle path-following control, our goal is to minimize the distance from the reference point c to the target path. Let e_L be the shortest distance on the ground plane from the reference point c to the target path, i.e., e_L is the distance from $c(X, Y)$ to $H(X_H, Y_H)$. Distance e_L is positive when the target path is on the right side of the bicycle and vice versa. Given the mathematic representation of the path, a number of methods can be used to calculate e_L such as Lagrange multipliers method [22]. From our bicycle riding experience, we can realize that the bicycle can be pushed towards the target path by leaning our body to the appropriate side. In Fig. 6, for instance, one can see that the bicycle is on the left of the path, or in other words, the path is on the right side of the rider (the presence of the rider is assumed). In order to reduce e_L , we need to lean towards to path, i.e., to the right. Using this strategy, we can design another controller to regulate to lean angle so that e_L is minimized. The magnitude of the lean angle is dependent on the distance e_L . Practice shows that, in order to retain the balance of the bicycle, the value of the lean angle θ should not be too large. In both control schemes, we restrict the range of θ_{ref} within $[-30^\circ, 30^\circ]$.

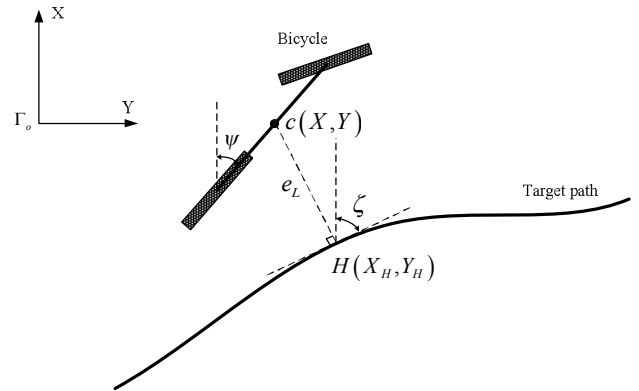


Fig. 6 Ground-path tracking strategy.

Control Scheme 1

In the first scheme, we design a fuzzy controller (FIS_{path_trkl}) that generates the corresponding θ_{ref} angle according to e_L and its change, Δe_L , until the error is

minimized. For path-tracking control, another control loop is added to the existing one given in Fig. 4. The control scheme is shown in Fig. 7. In facing the heading direction of the bicycle, θ is negative when the bicycle leans to the left and positive when it leans to the right. By considering the bicycle in the following three typical situations, the corresponding rules are discussed:

If e_L is -3 and Δe_L is -3, then θ_{ref} is -3:

This rule quantifies the situation wherein the bicycle is far from the target path and the target path is on the left of the bicycle. Hence, one should lean the bicycle to the left at a large angle to make the bicycle go to the left.

If e_L is 0 and Δe_L is 0, then θ_{ref} is 0:

This rule quantifies the situation wherein the bicycle is already in its proper position. No control effort is needed.

If e_L is 3 and Δe_L is 3, then θ_{ref} is 3:

In this case, the bicycle should be leaned to the right at a large angle to make the bicycle turn to the right.

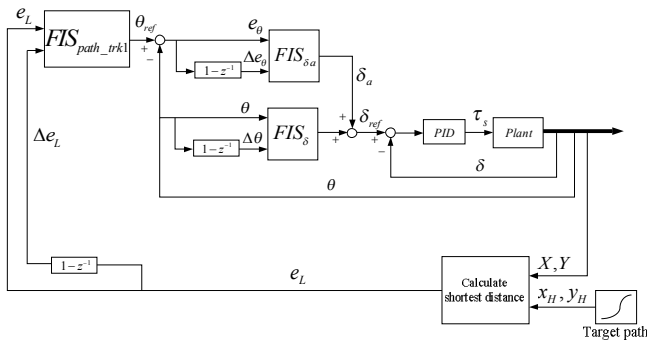


Fig. 7 Block diagram for path-following control using e_L and Δe_L for regulating roll-angle.

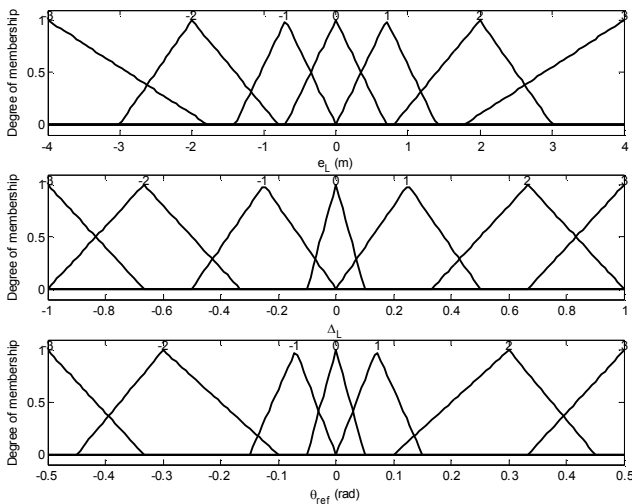
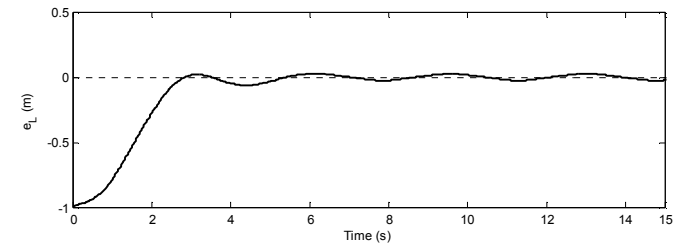
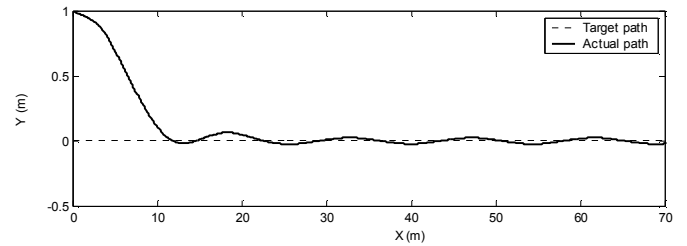
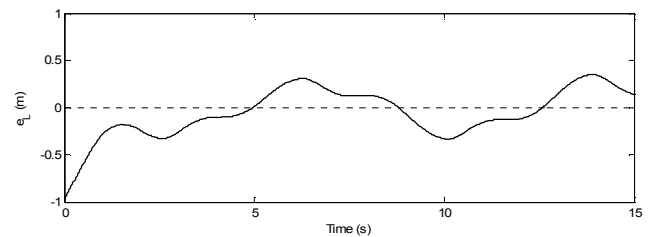
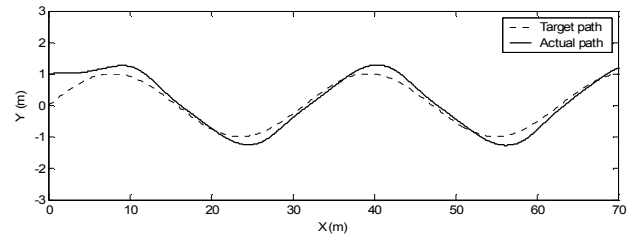


Fig. 8 Membership functions for FIS_{path_trk1} .

In a similar fashion, the complete rule-base is constructed as listed in Table 2. Notice that the body of the table lists the linguistic-numeric consequents of the rules, and the left column and top row of the table contain the linguistic-numeric premise terms. For this controller, with two inputs and seven linguistic values for each of these, there are at most $7^2 = 49$ possible rules. Note that we are using “-3” as an abbreviation for “negative large”, “-2” to represent “negative medium”, “-1” to represent “negative small” and “0” to represent “zero”. Similarly, “3”, “2” and “1” are used to represent “positive large”, “positive medium” and “positive small”, respectively.



(a)



(b)

Fig. 9 Trajectories of reference point c on ground-plane and tracking errors for following (a) a straight line and (b) a sinusoidal path $Y = \sin(0.2X)$ using control scheme 1.

the control inputs and output around zero are chosen to be relatively small.

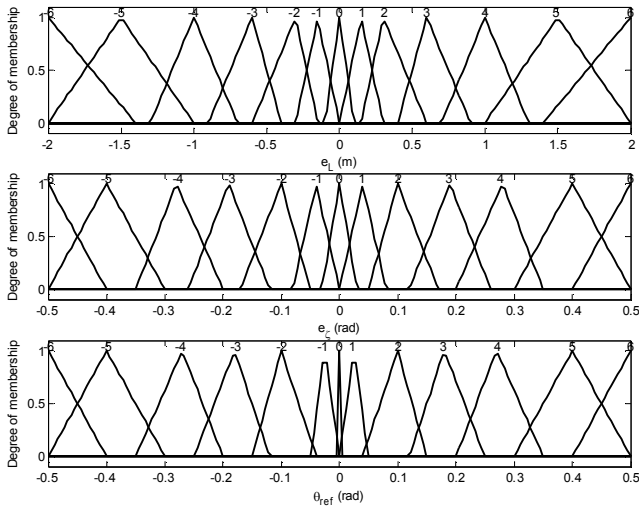


Fig. 11 Membership functions for FIS_{path_trk2} .

Table 3. Rule table for path-tracking for control scheme 2.

e_c	-6	-5	-4	-3	-2	-1	0	1	2	3	4	5	6
-6	0	1	2	2	3	3	4	4	5	5	6	6	6
-5	-1	0	1	2	2	3	3	4	4	5	5	6	6
-4	-2	-1	0	1	2	2	3	3	4	4	5	5	6
-3	-2	-2	-1	0	1	2	2	3	3	4	4	5	5
-2	-3	-2	-2	-1	0	1	2	2	3	3	4	4	5
-1	-3	-3	-2	-2	-1	0	1	2	2	3	3	4	4
0	-4	-3	-3	-2	-2	-1	0	1	2	2	3	3	4
1	-4	-4	-3	-3	-2	-2	-1	0	1	2	2	3	3
2	-5	-4	-4	-3	-3	-2	-2	-1	0	1	2	2	3
3	-5	-5	-4	-4	-3	-3	-2	-2	-1	0	1	2	2
4	-6	-5	-5	-4	-4	-3	-3	-2	-2	-1	0	1	2
5	-6	-6	-5	-5	-4	-4	-3	-3	-2	-2	-1	0	1
6	-6	-6	-6	-5	-5	-4	-4	-3	-3	-2	-2	-1	0

The effectiveness of this controller can be evaluated by a number of simulations. To make a comparison with the control scheme 1, two similar cases are shown. For straight line tracking as shown in Fig. 12a, the result has been improved a lot compared to the result shown in Fig. 9a and the steady state error converges to zero. By looking at Fig. 12b, it can also be

seen that the bicycle is able to track a sinusoidal path more closely with rather small overshoot. These results indicate that by utilizing human bicycle riding experience, the path-tracking problem can be solved more effectively.

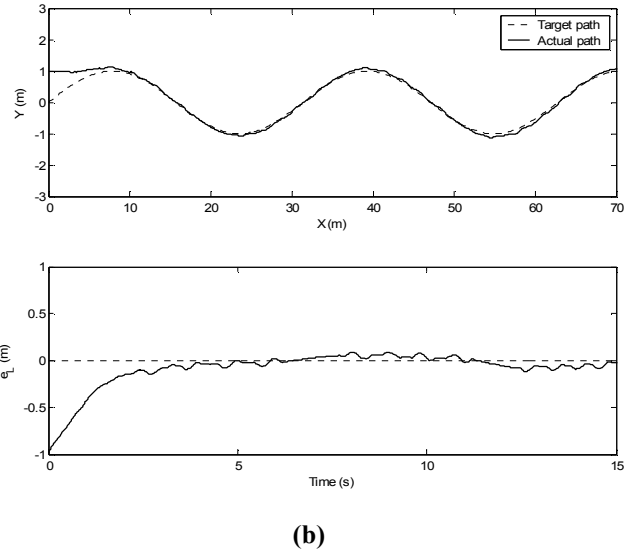
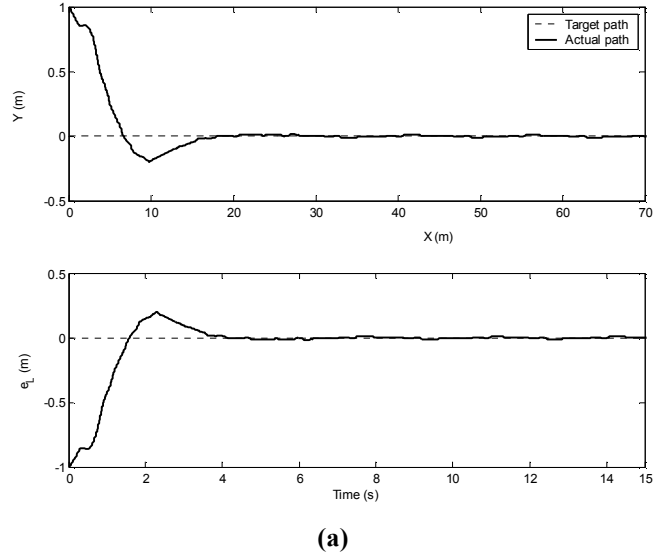


Fig. 12 Trajectories of reference point c on ground-plane and tracking errors for following (a) a straight line and (b) a sinusoidal path $Y = \sin(0.2X)$ using control scheme 2.

CONCLUSION

In this study, a nine-DOF dynamic model of an unmanned bicycle has been developed by using Lagrange's equations for quasi-coordinates. By considering the contact relationship between the two wheels and the ground plane, the constraint conditions, including four holonomic and four non-holonomic

ones, have been derived. According to this mathematical model, the fuzzy and PID controllers have been designed for stabilizing the bicycle in its straight-running motion and for roll-angle tracking while retaining balance. By considering the distance from the reference point c to the target path and the heading direction of the bicycle, two control schemes have been proposed and discussed for better understanding of interesting bicycle dynamic behaviors. The control schemes have also been confirmed by numerical tests. Future work will be continued with fuzzy controller parameters auto-tuning and associated problems.

ACKNOWLEDGMENT

The authors would like to thank the National Science Council of the Republic of China, Taiwan, for financially supporting this research under project number NSC 93-2213-E-212-037.

REFERENCES

- [1] Johns, D.E.H., 1970, "The Stability of the Bicycle," *Physics Today*, **23(4)**, American Institute of Physics, pp. 34-40.
- [2] Timoshenko, S., and Young, D.H., 1948, *Advanced Dynamics*, McGraw-Hill, New York, pp. 239-240.
- [3] Schwab, A.L., Meijaard, J.P., and Papadopoulos, J.M., 2004, "Benchmark Results on the Linearized Equations of Motion of an Uncontrolled Bicycle," *Proc. of the ACMD*, Korea, pp. 143-151.
- [4] Beznos, A.V., Formal'sky, A.M., Gurfinkel, E.V., Jicharev, D.N., Lensky, A.V., Savitsky, K.V., and Tchesalin, L.S., 1988, "Control of Autonomous Motion of Two-wheeled Bicycle with Gyroscopic Stabilization," *Proc. of the 1988 IEEE International Conference on Robotics & Automation*, **3**, Leuven, Belgium, pp. 2670-2675.
- [5] Han, S., Han, J., and Ham, W., 2001, "Control Algorithm for Stabilization of Tilt Angle of Unmanned Electric Bicycle," *Transaction on Control, Automation and Systems Engineering*, **3**, pp. 176-180.
- [6] Yavin, Y., 1999, "Stabilization and Control of the Motion of an Autonomous Bicycle by Using a Rotor for Tilt Moment," *Compute. Methods Appl. Mech. Engrg.*, **178**, pp. 233-243.
- [7] Getz, N.H., 1994, "Control of Balance for a Nonlinear Holonomic Non-minimum Phase Model of a Bicycle," *Proc. of the American Control Conference*, Baltimore, American Control Council.
- [8] Getz, N.H., and Marsden, J.E., 1995, "Control for an Autonomous Bicycle," *Proc. of the IEEE International Conference on Robotics and Automation*, **2**, pp. 1397-1402.
- [9] Getz, N.H., 1995, "Internal Equilibrium Control of a Bicycle," *Proc. of the 34th IEEE Conference on Decision and Control*, New Orleans, pp. 4285-4287.
- [10] Lee, S., and Ham, W., 2002, "Self Stabilizing Strategy in Tracking Control of Unmanned Electric Bicycle with Mass Balance," *Proc. of the 2002 IEEE/RSJ International Conference on Intelligent Robots and Systems*, **3**, pp. 2200-2205.
- [11] Chen, P.H., 2000, "A Scheme of Fuzzy Training and Learning Applied to Elebike Control System," *Proc. of the Ninth IEEE International Conference on Fuzzy Systems*, **2**, pp. 810-816.
- [12] Berriah, S., and Lachiver, G., 1999, "Control of Equilibrium and Trajectory of a Remotely Controlled Bicycle," *Proc. of the IEEE Canadian Conference on Electrical and Computer Engineering*, **2**, pp. 1014-1019 (in French).
- [13] Sharp, R.S., 1975, "The Dynamics of Single Track Vehicles," *Vehicle System Dynamics*, **5**, pp. 67-77.
- [14] Sharp, R.S., 1971, "The Control and Stability of Motorcycles," *J. Mech. Engng. Sci.*, **13(5)**, pp. 316-329.
- [15] Chen, C.K., Dao, T.S., and Yang, C.K., 2005, "Turning Dynamics and Equilibrium of Two-wheeled Vehicles," *J. of Mechanical Science and Technology*, **19(1)**, pp. 377-387.
- [16] Baruh, H., 1999, *Analytical Dynamics*, McGraw-Hill, Singapore.
- [17] Amirouche, F.M.L., 1992, *Computational Methods in Multibody Dynamics*, Prentice-Hall, New Jersey.
- [18] Shabana, A.A., 2001, *Computational Dynamics*, 2nd ed., John Wiley & Sons, New York.
- [19] Baumgarte, J., 1972, "Stabilization of Constraints and Integrals of Motion in Dynamics Systems," *Comput. Methods Appl. Mech. Eng.*, **1**, pp. 1-16.
- [20] Jeon, H., Choi, M.H., and Hong, M., 2004, "Numerical Stability and Convergence Analysis of Geometric Constraint Enforcement in Dynamic Simulation Systems," *Proc. of the MSV/AMCS 2004*, pp. 207-213.
- [21] Tanaka, Y., and Murakami, T., 2004, "Self Sustaining Bicycle Robot with Steering Controller," *The 8th IEEE International Workshop on Advanced Motion Control*, AMC '04, pp. 193-197.
- [22] Hubbard, J.H., and Hubbard, B.B., 2002, *Vector Calculus, Linear Algebra, and Differential Forms: a United Approach*, 2nd ed., Prentice Hall.